BOUND STATES IN CROSSOVER FROM THREE TO TWO DIMENSIONS USING FULLY CORRELATED GAUSSIAN BASIS

(Bundne tilstande i overgang fra tre til to dimensioner i fuldt korreleret Gaussisk basis)

Denmark, June 2016

Bachelor's Thesis
submitted by

Frederik Skovbo Møller
Stud. no.: 201303717
Department of Physics and Astronomy,
Aarhus University

Supervised by

Dmitri Vladimir Fedorov

Abstract

This thesis explores the dimensional crossover between three and two dimensions of two body bosonic systems interacting via a short-range potential and whether this transition can be described universally for any potential between the particles. The crossover is achieved by setting the particles in an external one dimensional harmonic oscillator trap, which confines the movement of the particles in the z-direction.

For determining the energies of the system, the stochastic variational method is used with a basis of fully correlated Gaussians. This allows description of non-spherical symmetric systems which is required for the one dimensional harmonic oscillator. The properties of the basis are tested by calculating both the spectrum of hydrogen and the splitting of energies when applying a magnetic field to a spinless hydrogen atom.

Calculating the binding energy of the two body system as function of the trap width for several interaction potentials displays how the transition is dependent on the shape and strength of the interactions. No universality is apparent except for the initial part of the crossover. However, choosing the length scale of the calculations as the effective range of the potentials and scaling the results accordingly reveals, that the weak-binding portion of the crossover is indeed universal.

Resumé

Dette projekt undersøger den dimensionale overgang mellem tre og to dimensioner for to-legeme bosoniske systemer, der interagerer via et kortrækkende potential, og hvorvidt denne overgang kan beskrives universelt for et vilkårligt potentiale mellem partiklerne. Overgangen opnås ved at placere partiklerne i en ekstern én-dimensional harmonisk oscillator fælde, som ved sammenpresning indskrænker partiklernes bevægelse i z-retningen.

For at bestemme energierne af systemet benyttes stokastisk variationsregning med en basis af fuldt korrelerede Gaussiske funktioner. Dette tillader beskrivelse af ikke-sfærisk symmetriske systemer, hvilket er påkrævet for den én-dimensionale harmoniske oscillator. Basens egenskaber testes ved at udregne både spektrummet af hydrogen samt det energisplit, som forekommer ved at udsætte et spinløst hydrogenatom for et magnetisk felt.

Udregningen af to-legeme systemets energi som funktion af vidden af fælden for adskillige interaktive potentialer viser, hvorledes overgangen er afhængig af form og styrke af interaktionerne. Ingen universalitet er tydelig bortset fra i den første del af overgangen. Ved at vælge den effektive rækkevidde af potentialerne som længdeskala og skalere resultaterne ifølge denne viser det sig dog, at en stor del af overgangen er universel.

Preface

This thesis concludes the three year long course of my bachelors degree. The thesis is weighted as 10 ECTS points, and the work involved in writing the necessary code, producing results and writing the paper has taken four months. For understanding the content of the thesis certain prerequisites are required. Thus, a basic understanding of atomic, nuclear and particle physics is expected as well as knowledge of quantum mechanics and linear algebra. Although the thesis contains a large amount of numerical computations, no prior knowledge to numerical methods is needed, as the necessary information is given in the thesis. However, for attempting to recreate the result some experience in programming and an understanding of numerical methods is advised.

I want to thank my supervisor Dmitri Fedorov for excellent guidance and for sharing knowledge about numerical methods and few body physics. Furthermore, I want to thank Stig Elkjær, who also did computations using the correlated Gaussian method, for discussing the properties and consequences of the method with me. Lastly, thanks to Filipe Bellotti for showing me results within dimensional crossover, and thanks to Alex Kalaee for sharing his LaTeX preamble.

Contents

Chapter 1

Introduction

In recent years a lot of work has been put into describing quantum physics in two dimensions. This is due to the number of spacial dimensions having a large significance on the dynamics of quantum systems. Thus, further exploration of the physics of two dimensions could produce results in fields such as ultracold gasses or superconductivity. One significant difference between the two and three dimensions is due to the centrifugal barrier operator, which in two dimensions has negative eigenvalues for zero angular momentum states. Hence, any infinitesimal attraction in two dimensions is sufficient to create a bound system [1].

In this thesis the crossover from three to two dimensions of a two particle system of bosons is examined. This is done by calculating the energies of the system using the correlated Gaussian method, which utilizes the variational principle with stochastic Gaussian functions as trial functions. Employing fully correlated Gaussians allows description of non-spherical symmetric systems. Both benefits and consequences of using a basis of fully correlated Gaussians is discussed throughout the thesis. Furthermore, the different dynamics of two dimensions is explained, and the effect of different potentials on the transitions between three and two dimensions is considered. The dimensional crossover is achieved by putting the particles in a one dimensional harmonic oscillator, which is being squeezed in one dimension. This confines the movement of the particles in one dimension but allows them to move freely in the remaining two dimensions.

Using the hydrogen system as reference the fully correlated Gaussian basis is tested for its capability of accurately describing a non-spherical symmetric system. Following this, the dimensional crossover is described for several interactive potentials between the particles. Lastly, the effective ranges of the potentials are calculated, and the crossover plot is scaled according to the effective ranges in order to examine whether the crossover is universal for any shape of the interactive potential.

Chapter 2

Mathematical description of the variational method

The variational method is an approach to estimate the energies of a physical system. The method allows approximation of both the ground state and exited states using arbitrary functions. Naturally a well chosen function will yield a more accurate result, however, the variational principle will give an upper bound for the energy of the desired state in any case. This chapter is based off theory described in Suzuki and Varga[2], where proofs for the following theorems can be found.

To illustrate this, consider a physical system with a Hamiltonian $\hat{H}$, which is time independent and bounded from below. The eigenvalue problems thus reads

$$\hat{H}\phi \;=\; E_n\phi \quad n = 1, 2, \ldots \tag{2.1}$$

where the eigenvalues E_n are assumed to be in order such that

$$E_1 \leq E_2 \leq \ldots \ . \tag{2.2}$$

Although the Hamiltonian of the system may be known, its eigenvalues and eigenvectors are often unknown. Due to the difficulty of actually solving the eigenvalue equation, it is in many cases more efficient to approximate to the solution. For this reason the variational method is extremely useful.
One of the key features of the variational principle is described in the *Ritz theorem.*

Theorem 2.1 (Ritz theorem) *For an arbitrary function Ψ of the state space the expectation value of $\hat{H}$ in the state Ψ is such that*

$$E \;\equiv\; \frac{\langle\Psi|\hat{H}|\Psi\rangle}{\langle\Psi|\Psi\rangle} \;\geq\; E_1 \ , \tag{2.3}$$

where the equality holds if and only if Ψ *is an eigenstate of* $\hat{H}$ *with the eigenvalue* E_1*.*

Hence, the expectation value of the Hamiltonian taken with an arbitrarily chosen function will yield an upper bound for the ground state energy. By choosing "good" functions, the deviation from E_1 becomes minimal. However, the approximation may only be exact for the eigenfunction itself.
The variational principle is not restricted to ground state approximations. In order to describe exited states, a linear combination of independent functions is often used

$$\Psi \;=\; \sum_{i=1}^{K} c_i \psi_i \;. \tag{2.4}$$

Although the functions have to be linear independent, they are not required to be mutually orthogonal. For non-orthogonal functions (E.g the Gaussian functions used in the correlated Gaussian method) the overlap is not unit. Thus, the eigenvalue problem of equation 2.1 becomes a general eigenvalue problem. The functions $\psi_1, \ldots, \psi_K$ spans the subspace V_K, thus restricting the eigenvalue problem to said subspace, which in many cases is an advantage.

Theorem 2.2 (Mini-Max theorem) *Let* $\hat{H}$ *be a Hermitian operator with discrete eigenvalues* $E_1 \leq E_2 \leq \ldots$*. Let* $\epsilon_1 \leq \epsilon_2 \leq \ldots \leq \epsilon_K$ *be the eigenvalues of* $\hat{H}$ *restricted to the subspace* V_K *of a linearly independent set of K functions* $\psi_1, \ldots, \psi_K$*. Then*

$$E_1 \leq \epsilon_1,\; E_2 \leq \epsilon_2,\; \ldots,\; E_K \leq \epsilon_K \;. \tag{2.5}$$

Using a linear combination of linear independent functions thus allows for approximation of the ground state plus an additional $K-1$ excited states. Restricting the problem to a subspace V_K has several advantages. One of them is the ability to increase the precision of the approximated eigenvalues by expanding the basis. Hence, higher precision can be achieved through either better trial functions ψ_i, an increase in basis size K, or a combination of both. The following theorem describes the consequences of increasing the basis size.

Theorem 2.3 *Let* $\epsilon_1 \leq \epsilon_2 \leq \ldots \leq \epsilon_K$ *be the eigenvalues of a Hermitian operator* $\hat{H}$ *restricted to the subspace* V_K *of linear combinations*

of independent functions $\psi_1, \ldots, \psi_K$. *Let* $\epsilon'_1 \leq \epsilon'_2 \leq \ldots \leq \epsilon'_{K+1}$ *be the eigenvalues of* $\hat{H}$ *restricted to the subspace* V_{K+1} *of linear combinations of independent functions* $\psi_1, \ldots, \psi_K, \psi_{K+1}$. *Then*

$$\epsilon'_1 \leq \epsilon_1 \leq \epsilon'_2 \leq \epsilon_2 \leq \ldots \leq \epsilon'_K \leq \epsilon_K \leq \epsilon'_{K+1} \,. \tag{2.6}$$

An expansion of the basis will not worsen the previously calculated eigenvalues. Therefore, expanding the basis can be done without worry of loss of precision. Since this applies to all the previously calculated eigenvalues, one may find that improving the approximation of the energy of a higher exited state may yield better results for all lower lying states. In the limiting case of the subspace approaching the full Hilbert space, all the eigenvalues of the restricted subspace will converge to the exact eigenvalues of the Hamiltonian [2]. Thus, theorem 2.3 in principle implies the Mini-Max Theorem.

In practice increasing the basis size for higher precision is not always a viable strategy. This is mainly due to the system becoming overdetermined causing numeric eigenvalues algorithm to produce round-off errors, thus reducing precision. Furthermore, a larger basis requires more computations. When determining the eigenvalues of a system, one has to weigh precision against time spent, and depending on the system only a small basis may be required for accurate results.

Chapter 3

The correlated Gaussian method

In the correlated Gaussian method stochastic generated Gaussian functions are used as trial function for approximating the eigenenergies of a system. The method is based on the principles of the variational method and offers the advantage of easily calculated matrix elements.

3.1 The generalized eigenvalue problem

Because Gaussians are generally not orthogonal, their overlap will not be diagonal. A consequence of this is a generalized eigenvalue problem. Consider the eigenvalue problem

$$\hat{H}|\Psi\rangle = E|\Psi\rangle \ , \tag{3.1}$$

in which E and $|\Psi\rangle$ are considered the true eigenvalue and eigenfunction of the Hamiltonian. Next, consider a function $|\phi_k\rangle$ from the subspace V_K of the chosen basis functions. Inserting $|\phi_k\rangle$ into equation 3.1 yields

$$\hat{H}|\phi_k\rangle = \epsilon_k|\phi_k\rangle \ , \tag{3.2}$$

where ϵ_k is the energy corresponding to the state $|\phi_k\rangle$. As $|\phi_k\rangle$ is part of the subspace of the basis, it can be represented as a linear combination of the basis functions $|\psi_i\rangle$. Thus, equation 3.2 reads

$$\hat{H}\sum_{i=1}^{K} c_{k,i}|\psi_i\rangle = \epsilon_k \sum_{i=1}^{K} c_{k,i}|\psi_i\rangle \ . \tag{3.3}$$

Now, projecting equation 3.3 onto an arbitrary basis function $|\psi_j\rangle$ for the subspace V_K results in

$$\sum_{i=1}^{K} c_{k,i}\langle\psi_j|\hat{H}|\psi_i\rangle = \epsilon_k \sum_{i=1}^{K} c_{k,i}\langle\psi_j|\psi_i\rangle \ . \tag{3.4}$$

This expression can be written much more compactly in matrix form by defining the matrix elements

$$\mathcal{H}_{j,i} \equiv \langle \psi_j | \hat{H} | \psi_i \rangle \quad , \quad \mathcal{B}_{j,i} \equiv \langle \psi_j | \psi_i \rangle \ . \tag{3.5}$$

From these elements equation 3.4 can be written as

$$\mathcal{H}\boldsymbol{c_k} = \epsilon_k \mathcal{B}\boldsymbol{c_k} \ , \tag{3.6}$$

which is a generalized eigenvalue problem.
Through Cholesky decomposition the problem can be reduced to an ordinary eigenvalue problem. In the Cholesky decomposition of the overlap matrix, $\mathcal{B}$, it is written as a product of lower triangular matrix L and its transposed

$$\mathcal{B} = LL^T \ . \tag{3.7}$$

For the decomposition, it is a requirement that $\mathcal{B}$ is positive definite. However, $\mathcal{B}$ is a Gram-matrix, meaning its entries are inner products of a set of vectors. Therefore, it is positive definite by definition [3]. Inserting the decomposition 3.7 into the generalized eigenvalue problem 3.6 allows the rewriting

$$\begin{aligned} \mathcal{H}\boldsymbol{c_k} &= \epsilon_k LL^T \boldsymbol{c_k} \quad \Leftrightarrow \\ L^{-1}\mathcal{H}(L^T)^{-1}L^T\boldsymbol{c_k} &= \epsilon_k L^T \boldsymbol{c_k} \quad \Leftrightarrow \\ \mathcal{H}'\boldsymbol{c_k}' &= \epsilon_k \boldsymbol{c_k}' \ . \end{aligned} \tag{3.8}$$

The generalized eigenvalue problem has thus been transformed into a regular eigenvalue problem without modifying the eigenvalues ϵ_k.

3.2 Selection of coordinates for the system

Using the right set of coordinates for the system at hand can often simplify calculations. In this instance it is the inner structure of a system of particles that is of interest. Thus, using relative coordinates allows for separation of the center of mass coordinate, which can be neglected in any computations regarding the relative positions of the particles. As a result a system of N bodies can be described by a set

of independent, relative coordinates $\{\boldsymbol{x_1}, \ldots, \boldsymbol{x}_{N-1}\}$.
For this a linear coordinate transformation is used

$$\tilde{\boldsymbol{x}} = \mathcal{U}\tilde{\boldsymbol{r}} \,, \tag{3.9}$$

where $\tilde{\boldsymbol{r}}$ is the coordinate vectors of the N particles, and $\mathcal{U}$ is the transformation matrix. The tilde abbreviates a super vector, which is a vector containing other vectors. Thus, $\tilde{\boldsymbol{x}}$ is the vector containing all the relative coordinate vectors

$$\tilde{\boldsymbol{x}} \equiv \begin{pmatrix} \boldsymbol{x}_1 \\ \vdots \\ \boldsymbol{x}_N \end{pmatrix} . \tag{3.10}$$

The transformation matrix can be chosen in several ways following certain criteria which allows for easier calculations: Firstly, the final row of $\mathcal{U}$ is chosen such that $\boldsymbol{x}_N$ is the center of mass coordinate. Secondly, if the matrix is unitary, the diagonal form of the kinetic energy and the harmonic trap is preserved in the new coordinates [4]

$$T = -\frac{\hbar^2}{2m} \sum_i \frac{\partial}{\partial \boldsymbol{x}_i^2} \tag{3.11}$$

$$V_h = \frac{m\omega^2}{2} \sum_i \boldsymbol{x}_i^2 \,. \tag{3.12}$$

With these considerations in mind the transformation matrix was chosen as [2]

$$\mathcal{U} = \begin{pmatrix} 1 & -1 & 0 & \ldots & 0 \\ \frac{m_1}{m_1+m_2} & \frac{m_2}{m_1+m_2} & -1 & \ldots & 0 \\ \vdots & \vdots & \vdots & \ddots & \vdots \\ \frac{m_1}{m_1+\ldots+m_N} & \frac{m_2}{m_1+\ldots+m_N} & \ldots & \ldots & \frac{m_N}{m_1+\ldots+m_N} \end{pmatrix} . \tag{3.13}$$

The resulting coordinate of using the matrix 3.13 is a set of *Jacobi coordinates*.

Choosing a transformation matrix such as $\mathcal{U}$ allows separation of the internal motion from the motion of the center of mass, which was among the desired effects of changing coordinates. Applying the

inverse of the transformation 3.9 upon the momentum operator yields [2]

$$\boldsymbol{p}_{i,r} = \sum_{j=1}^{N} \mathcal{U}_{ji} \boldsymbol{p}_{j,x} = \frac{\hbar}{i} \sum_{j=1}^{N} \mathcal{U}_{ji} \frac{\partial}{\partial \boldsymbol{x}_j} \ . \tag{3.14}$$

Knowing this the total kinetic energy operator can be written as [5]

$$\begin{aligned} -\sum_{i=1}^{N} \frac{\hbar^2 \boldsymbol{p}_{i,r}^2}{2m_i} &= -\frac{\hbar^2}{2} \sum_{i=1}^{N} \frac{1}{m_i} \left(\sum_{k=1}^{N} \mathcal{U}_{ki} \frac{\partial}{\partial \boldsymbol{x}_k} \right) \left(\sum_{j=1}^{N} \mathcal{U}_{ji} \frac{\partial}{\partial \boldsymbol{x}_j} \right) \\ &= -\frac{\hbar^2}{2} \sum_{k=1}^{N-1} \sum_{j=1}^{N-1} \sum_{i=1}^{N} \frac{\mathcal{U}_{ki}\mathcal{U}_{ji}}{m_i} \frac{\partial}{\partial \boldsymbol{x}_k} \frac{\partial}{\partial \boldsymbol{x}_j} - \frac{\hbar^2}{2} \sum_{i=1}^{N} \frac{\mathcal{U}_{Ni}^2}{m_i} \frac{\partial}{\partial \boldsymbol{x}_N^2} \\ &= -\frac{\hbar^2}{2} \sum_{k=1}^{N-1} \sum_{j=1}^{N-1} \Lambda_{kj} \frac{\partial}{\partial \boldsymbol{x}_k} \frac{\partial}{\partial \boldsymbol{x}_j} - \frac{\hbar^2}{2(m_1 + \ldots + m_N)} \frac{\partial}{\partial \boldsymbol{x}_N^2} \\ &= \hat{T}_{int} + \hat{T}_{CM} \ , \end{aligned} \tag{3.15}$$

where $\hat{T}_{int}$ and $\hat{T}_{CM}$ denotes the kinetic energy operator of the internal system and the center of mass respectively. Furthermore, the matrix elements Λ_{kj} are defined as

$$\Lambda_{kj} \equiv \sum_{i=1}^{N} \frac{\mathcal{U}_{ki}\mathcal{U}_{ji}}{m_i} \ , \tag{3.16}$$

such that Λ, in the case of the transformation matrix 3.13, is a diagonal matrix containing inverses of the reduced masses of the jacobi subsystems. Finally, in the derivation of equation 3.15 the relation

$$\sum_{i=1}^{N} \mathcal{U}_{ji} = \delta_{N,i} \tag{3.17}$$

was used, where δ is the delta function. Equation 3.17 can easily be seen from the transformation matrix 3.13, as each row sums to zero besides the N'th, which sums to one.

3.3 Description of the basis

As stated in the Ritz theorem, theorem 2.1, any arbitrary function can be chosen as part of the basis. However, when choosing types of

functions one should consider the properties of said functions. Firstly, the matrix elements specified in equation 3.5 should be easy to calculate analytically. Secondly, the functions should be flexible enough to account for any number of bodies described and for rapidly varying functions. Gaussian functions fit all of these criteria.

Mainly there are two types of Gaussian bases, which are used for stochastic variational methods: Spherical symmetric Gaussians and fully correlated Gaussians. For spherical symmetric Gaussians each coordinate vector consists only of a single value, namely the radial length. This allows for smaller basis functions, hence lower computation times. In fully correlated Gaussians, however, each coordinate vector holds Cartesian coordinates. While this causes the basis functions to be much larger, it also allows much more flexibility of the functions.
In general the Gaussian basis functions can be described as

$$|A, s; x\rangle \equiv \exp\left(-\sum_{i,j=1}^{D\cdot n} A_{ij}(\tilde{\boldsymbol{x}}_i - \tilde{\boldsymbol{s}}_i)(\tilde{\boldsymbol{x}}_j - \tilde{\boldsymbol{s}}_j)\right) = e^{-(\tilde{\boldsymbol{x}}-\tilde{\boldsymbol{s}})^T A(\tilde{\boldsymbol{x}}-\tilde{\boldsymbol{s}})}\,. \tag{3.18}$$

Here $n = N-1$ is the amount of relative coordinate vectors, and D is the dimensionality of the system. In order to obtain fully correlated Jacobi coordinates, the transformation matrix 3.13 has to be modified such that every entry is a diagonal, square matrix of size D. The shift vector $\tilde{\boldsymbol{s}}$ allows for some additional flexibility of the basis functions. These vectors are especially important when describing non-spherical symmetric states.

3.4 Optimization of the basis

When selecting parameters for a new trial function for the variational method, several approaches can be taken. However, in this instance stochastic chosen parameters were used. Stochastic variational method has the advantage of not converging towards a local minima, which may be very common in more complex systems. Thus, with enough stochastic samples the algorithm will almost surely converge towards the global minima. The coefficients of the matrix A

from equation 3.18 were chosen as

$$A_{ij} = \delta_{i,j}/b_i^2 \ , \tag{3.19}$$

where b_i is stochastically sampled from an exponential distribution, and $\delta_{i,j}$ is the delta function. As a result A is diagonal, which is preferable for systems with spherical symmetries. For more complex systems, however, A may be scrambled by taking the matrix product $A' = Q^T A Q$, where Q is from a QR-factorization of a randomly generated matrix. Doing this will conserve the properties of the matrix A. The shift vectors $\tilde{\boldsymbol{s}}$ were also sampled from an exponential distribution.

When optimizing upon the basis two methods were employed: Expansion of basis and refinement of basis. For the refinement of the basis, one function of the basis is selected and temporarily replaced with randomly generated functions. If either of these functions yield a lower energy, the original basis function is replaced. This process continues for the remaining basis functions and can be cycled through the entire basis multiple times for increased effect. Optimization of the basis may also be achieved through expansion of the basis as described by theorem 2.3.

In this instance a combination of refinement loops and basis expansion was used. For the ground state a suitable basis size was chosen, and through several loops of refinement this basis was optimized for describing the ground state. Thereafter, the exited states were approximated by expanding the basis. The advantage of this method is the ease of improving upon a previously calculated result by simply adding more basis functions. Furthermore, the initial refinement loops allows a good approximation of the ground state without using a large basis. This reduces runtime, as calculations become more time consuming with a larger basis.

As mentioned earlier Gaussians are not orthogonal. While this causes some additional calculations due to their overlap, it also has some nice properties. For instance one does not have to ensure that a newly generated function is orthogonal to the remaining basis [2]. Thus, trial functions can be generated and chosen faster and easier, therefore increasing the efficiency of the stochastic variational method.

3.5 Consequences of full correlation

Determining which type of Gaussian to use for solving a given problem is very important, as this choice will have great impact on the efficiency and flexibility of the variational method. As stated earlier, spherical symmetric Gaussians requires fewer calculations than fully correlated Gaussians. To illustrate this, consider the calculation of the elements of the overlap matrix. The bottleneck of these computations lies in taking the determinant of a matrix of size equal to that of the A-matrices of the Gaussians (see appendix equation A.3). The determinant can be computed through LU-decomposition and requires $O(n^3)$ computation [6], where n is the size of the given matrix. Since fully correlated Gaussians have coordinates for every Cartesian coordinate of the space of the system, their A-matrices will be of dimensions $(N-1)D \times (N-1)D$. This is a factor D larger than for spherical Gaussians. Since the systems in this instance will be three dimensional, taking the determinant with a fully correlated basis requires $3^3 = 27$ times more computations than for spherical Gaussians. Furthermore, one has to consider the larger amount of parameters to be optimized for correlated Gaussians. Thus, it should come as no surprise, that the time of convergence for simple systems of high symmetry is much lower when using spherical Gaussians. However, a fully correlated Gaussians basis allows much more versatility in the systems described. Furthermore, it enables description of systems with distinct spatial directions.

In theory fully correlated Gaussians should be able to describe all systems without the use of shift vectors. Shift vectors allows a spherical Gaussian to describe non-spherical symmetric states. However, shift vectors are also necessary for describing certain exited states in a fully correlated basis. Consider the parity operator $\hat{P}$,

$$\hat{P}\varphi(\boldsymbol{x}, t) \equiv P\varphi(-\boldsymbol{x}, t) \ , \tag{3.20}$$

where $P = \pm 1$ is the eigenvalues of the operator [7]. Gaussian functions have their coordinates squared, and since the Hamilton operator does not affect the eigenfunction the following relation is true:

$$\langle A, s; x|\hat{H}|A, s; x\rangle = \langle A, s; -x|\hat{H}|A, s; -x\rangle \ . \tag{3.21}$$

Therefore, without the shift fully correlated Gaussians are unable to describe states with odd angular momentum quantum number l.

Chapter 4

Bound states in dimensional crossover

4.1 Centrifugal barrier in two dimensions

Transitioning from three to two dimensions will have an effect on the centrifugal barrier operator. In three dimensions the centrifugal barrier eigenvalues will assume values that are positive or zero, thus opposing a binding of the particles. In two dimensions, however, the eigenvalues are negative for zero angular momentum. Thus, an infinitesimal attraction between particles will be sufficient to cause a bound system [1]. Consider the kinetic energy operator in two dimensions

$$\hat{T}_{2D} = -\frac{\hbar^2}{2m}\nabla^2 = -\frac{\hbar^2}{2m}\left(\frac{\partial^2}{\partial x^2} + \frac{\partial^2}{\partial y^2}\right) . \tag{4.1}$$

Rewriting the operator in polar coordinates and applying it to a function $f(r)$ yields

$$\hat{T}_{2D} f = -\frac{\hbar^2}{2m}\left(\frac{\partial^2 f}{\partial r^2} + \frac{1}{r}\frac{\partial f}{\partial r} + \frac{1}{r}\frac{\partial^2 f}{\partial \phi^2}\right) = \varepsilon f . \tag{4.2}$$

Consider the function f representing a state with zero angular momentum, hence its derivative with respect to ϕ being zero. Furthermore, f is of the form $f(r) = r^n u(r)$, whereby equation 4.2 reads

$$-r^n\frac{\partial^2 u}{\partial r^2} - r^{n-1}\frac{\partial u}{\partial r}(2n+1) - r^{n-2}u(n(n+1)+n) = \frac{2m\varepsilon}{\hbar^2}r^n u . \tag{4.3}$$

Choosing $n = -\frac{1}{2}$ implies $\int |f|^2 \mathrm{d}^2x = \int |u|^2 \mathrm{d}r \int \mathrm{d}\phi$. Dividing by r^n in equation 4.3, inserting $n = -\frac{1}{2}$, and rearranging the terms allows

writing it in the form

$$-\frac{\hbar^2}{2m}\left(\frac{\partial^2 u}{\partial r^2}-\frac{1}{4r^2}u\right)=\varepsilon u\ . \tag{4.4}$$

The term $\frac{\hbar^2}{2m}\frac{1}{4r^2}$ is the centrifugal barrier, which, as stated earlier, has the opposite sign of its three dimensional counterpart. This centrifugal barrier is a consequence of the system being two dimensional and will only act as an effective potential. Thus, it will not lead to the binding of particles on its own, however, any infinitesimal attraction between the particles will cause them to create a bound system [1].

4.2 Squeezing of harmonic oscillator

An advantage of the fully correlated basis is the ability to actively adjust the potential in a single direction. This allows investigation of quantum systems in the transition from three to two dimensions. To achieve this, the particles are placed in a harmonic oscillator in the z-direction

$$V_{osc}=\frac{1}{2}m\omega^2 z^2=\frac{1}{2}\frac{\hbar^2}{mb_{osc}^2}\frac{z^2}{b_{osc}^2}\ , \tag{4.5}$$

where b_{osc} is considered the width of the oscillator. In the limit of $b_{osc}\to\infty$ the strength of the oscillator becomes negligible, and the particles will behave as if they were free. However, in the limit of $b_{osc}\to 0$ the particles will effectively be trapped in the xy-plane. Thus, the effect of the dimensional crossover from three to two dimensions can be analysed by calculating the energies of the system for varying lengths of b_{osc}.

In order to actually see the formation of a bound system, it is necessary to separate the oscillator potential of the center of mass from that of the internal system. As seen in equation 3.15 the kinetic energy operator could be split into a term involving the center of mass and a term involving the internal motion. Likewise can be done for the harmonic oscillator. Hence, the Hamilton of the system can be split into a term for the internal system and for the center of mass, which allows describing the two systems separately. Thus, the eigenvalue problem for the center of mass reads

$$(\hat{T}_{CM}+\hat{V}_{osc,CM})\psi_0=\frac{1}{2}\hbar\omega\psi_0\ . \tag{4.6}$$

Therefore, separating the center of mass coordinate from the remaining Jacobi coordinates in equation 4.5 allows for description of the internal system (see Appendix A.4). Furthermore, the expectation value of the harmonic oscillator has to be subtracted from the result in order to see the effect of the squeezing. Otherwise, as b_{osc} becomes small, the potential energy of the oscillator grows huge thus overshadowing the effect of the dimensional crossover.

The squeezing of harmonic oscillators can in fact be done experimentally. For this an optical lattice is used, where counter propagating laser beams trap the atoms in a dipole potential. This is done by inducing an oscillating dipole moment in the atom, through the oscillating electric field of the laser. The same field interacts with the induced dipole moment to create the desired potential. The actual lattice is formed by interfering multiple laser beams, often to create a periodic, "egg tray" like potential. The actual squeezing is achieved by adjusting the intensity of the laser beams, which determines the dipole potential. [8]

4.3 Effective range

One point of interest is the energy of a system during the dimensional crossover and how it is affected by the interactive potential between the particles. During squeezing the average distance between particles shortens, hence the expectation value of the interactive potential should change. Therefore, scaling different interaction potentials in correlation with some physical parameter could result in a universal dimensional transitions for all potentials. This physical parameter could be the effective range of the potentials. [9]

The effective range theory describes nucleon scattering in the low-energy regime. For kinetic energies lower than the potential, the theory allows the scattering to be determined by only two parameters: the *scattering length* a, and the *effective range* R [10]. To see this consider the Schrödinger equation for a radial wave function $u(r)$ with zero angular momentum,

$$\frac{\mathrm{d}^2 u}{\mathrm{d}r^2} + \left(k^2 - \frac{2V\mu}{\hbar^2}\right) u = 0 \,, \tag{4.7}$$

where $k = \sqrt{2\mu E/\hbar^2}$, μ is the reduced mass, and V is the potential. For large distances the potential will go towards zero, while

$$u_k(r) \to C\sin(kr + \delta) \ , \tag{4.8}$$

where $C = \frac{1}{\sin\delta}$ is a normalization constant. Next, consider the free-scattering wave function, $\tilde{u}_k$, which is the equivalent wave function for zero interaction. The asymptotic behaviour of $\tilde{u}_k$ for large distances is identical to that of u_k, since the potential at these distances is zero. By multiplying wave functions for two different values of k, solving the Schrödinger equation and subtracting the results, it can be shown that [10]

$$k_2\cot\delta_2 - k_1\cot\delta_1 = (k_2^2 - k_1^2)\int_0^\infty (\tilde{u}_1\tilde{u}_2 - u_1u_2)\mathrm{d}r \ , \tag{4.9}$$

Taking $k_1 = 0$ and $k_2 = k$ yields

$$k\cot\delta = \frac{1}{a} + \frac{1}{2}k^2R(k) \ , \tag{4.10}$$

where $R(k)$ is the desired effective range, which is given as

$$R(k) = 2\int_0^\infty (\tilde{u_0}\tilde{u_k} - u_0u_k)\mathrm{d}r \ . \tag{4.11}$$

In the low energy regime where $E < V$, the difference between u_k and u_0 will be very small. Therefore, the free-scattering wave functions will be similar as well, which allows the approximation [10]

$$R(k) \approx R(0) = 2\int_0^\infty (\tilde{u}_0^2 - u_0^2)\mathrm{d}r \ . \tag{4.12}$$

The mathematical description of the effective range emphasizes why it may be a useful scaling parameter. Since the free-scattering wave function is equal to the original wave functions outside the influence of the potential, the integrand of equation 4.12 vanishes for larger values of r. Therefore, the main influence on the value of the effective range is how far the potential extends. Thus, potentials of comparable range should have comparable effective ranges. As particles are squeezed together, the energy of their system is dependent on how much the particles interact. Hence, a system with a longer range interactive potential should during a dimensional crossover display different characteristics than if it had a potential of shorter range. Thus, scaling the potentials with their effective range might cause the transition to appear very similar for different potentials.

Chapter 5

Testing the method

In order to simplify the numeric calculations it is an advantage to choose a suitable set of units. For evaluating the hydrogen system atomic units (a.u.) are very convenient. In atomic units the electron mass, the elementary charge, Plancks reduced constant and Coulombs constant is set to unity

$$m_e = e = \hbar = k_e = 1 \text{ a.u. .} \tag{5.1}$$

This has the favourable consequence of simplifying several quantities present in the numerical computations:

$$a_0 = \frac{4\pi\varepsilon_0\hbar^2}{m_e e^2} = 1 \text{ a.u.} \tag{5.2}$$

$$E_0 = -\frac{m_e}{2\hbar^2}\left(\frac{e^2}{4\pi\varepsilon_0}\right)^2 = -\frac{1}{2} \text{ a.u.} \tag{5.3}$$

$$\mu_B = \frac{e\hbar}{2m_e} = \frac{1}{2} \text{ a.u. ,} \tag{5.4}$$

here a_0 being the Bohr radius, E_0 being the hydrogen ground state energy, and μ_B being the Bohr magneton.

Whether the optimization algorithm achieves good results may depend on the stochastic sampling of the parameters, i.e. b_i from equation 3.19. The mean of the distribution is chosen as the expectation value of r with respect to the Gaussian function $\psi_\gamma = \exp\left(-\frac{1}{2}\gamma r^2\right)$ [2]

$$\langle\psi_\gamma|r|\psi_\gamma\rangle = \sqrt{\frac{4}{\pi\gamma}} \,. \tag{5.5}$$

For hydrogen the mean parameter is set as $\gamma = \frac{4}{\pi}$, since the Bohr radius is unity. The spin of the electron and the nucleus is not considered in the calculations.

5.1 Expansion of coulomb potential

The hydrogen atom is analytically solvable due to the Coulomb attraction being a central force. Thus, the hydrogen wave function can be split into a radial and an angular part [11]. Unfortunately this is not possible in a fully correlated basis, as $V_C \propto \frac{1}{r}$, which can not be split into its Cartesian components. As a solution the Coulomb potential can be expanded in a series of Gaussian functions. Choosing the unit of length as the Bohr radius a_0 prompts the following expansion

$$\frac{a_0}{r} \simeq \sum_{k=1}^{G} \beta_k \exp\left(-\frac{r^2}{\alpha_k^2}\right). \tag{5.6}$$

One method of determining β_k and α_k is sampling the parameters from a given distribution. In this instance α_k was sampled with a logarithmic spacing in the range α_{min} to α_{max}. Following this the values of β_k were obtained by solving equation 5.6 for N_r values of r. The logarithmic distribution was chosen, as $1/r$ varies fast for small values of r, thus prompting a higher density of Gaussians compared to higher values, where variations are slow. The parameters α_{min} and α_{max} were found in [12] through calculations of the hydrogen ground state energy, which yielded $\alpha_{min} = 0.01$ and $\alpha_{max} = 10$. However, replicating those calculations using the logarithmic distribution led to better convergence for a slightly wider interval, namely $\alpha_{min} = 0.005$ and $\alpha_{max} = 12$.

Calculating the expectation value of the Coulomb potential is done in a similar manner to calculating the overlap. The process is illustrated in Appendix A.2. Unfortunately the calculations involve taking a determinant for every Gaussian in the expansion. Hence, computations involving the Coulomb potential in a fully correlated basis are very slow, as taking the determinant is a heavy computational operation.

Finally, increasing the amount of Gaussians in the expansion, G, will not always yield a better result. Although the fidelity may become lower, the resulting expansion will consist of Gaussians with very large values of β_k and with alternating sign. Such an expansion will be prone to round-off errors, thus leading to a poor result. Therefore, an expansion of size $G = 10$ was chosen, as this was sufficient for producing accurate results while maintaining a reasonable runtime.

5.2 The hydrogen atom

The *Ritz Theorem*, theorem 2.1, states that only the eigenfunction of the Hamiltonian will yield the exact eigenvalue. Thus, as the approximated energy approaches the eigenvalue so should the linear combination of Gaussian functions approach the wavefunction. Therefore, other expectation values than the energy should resemble those of hydrogen. The r^2 operator commutes with the Hamiltonian [11], thus it will have the same eigenstates as those of the Hamiltonian. Therefore, $\langle r^2 \rangle$ can be calculated using the approximated wave function. If the expectation values of both $\hat{H}$ and $\hat{r}^2$ are comparable with theoretical values, the linear combination of basis functions resembles the hydrogen wave function.

For calculating the energies of hydrogen a basis size of $K = 8$ was chosen for the ground state, as this allowed for decent precision while maintaining a relatively low runtime. The basis was optimized through 3 refinement loops with 5000 trial functions for each basis function. The exited states were calculated by expanding the basis. For the i'th state $6 + i$ functions were added to the basis size, and each member was chosen using 10000 trial functions. In total five states were optimized, although an additional two were calculated in order to display further exited states.

The results of the calculations for the first 5 states can be seen in table 5.1, and a visual of the approximated energies, $\mathrm{E_{app}}$, can be seen in figure 5.1.

Only the ground state improves when optimizing it through refinement loops, while all states are improved when expanding the basis. After three refinement loops the approximated ground state energy has almost converged to the theoretical value $\mathrm{E_{gs}}$. The highest exited states are quite imprecise, as the initially chosen parameters are better suited for the lower exited states. However, the two higher exited states were included primarily as a visual, hence they are not listed in table 5.1.

As seen from table 5.1 the correlated Gaussian basis is able to reproduce the energy spectrum of the hydrogen atom within single digit percentile deviation. Furthermore, the basis is sufficient for calculating $\langle r^2 \rangle$, although the deviation is larger compared to that of the energies. Further precision could be achieved with more basis

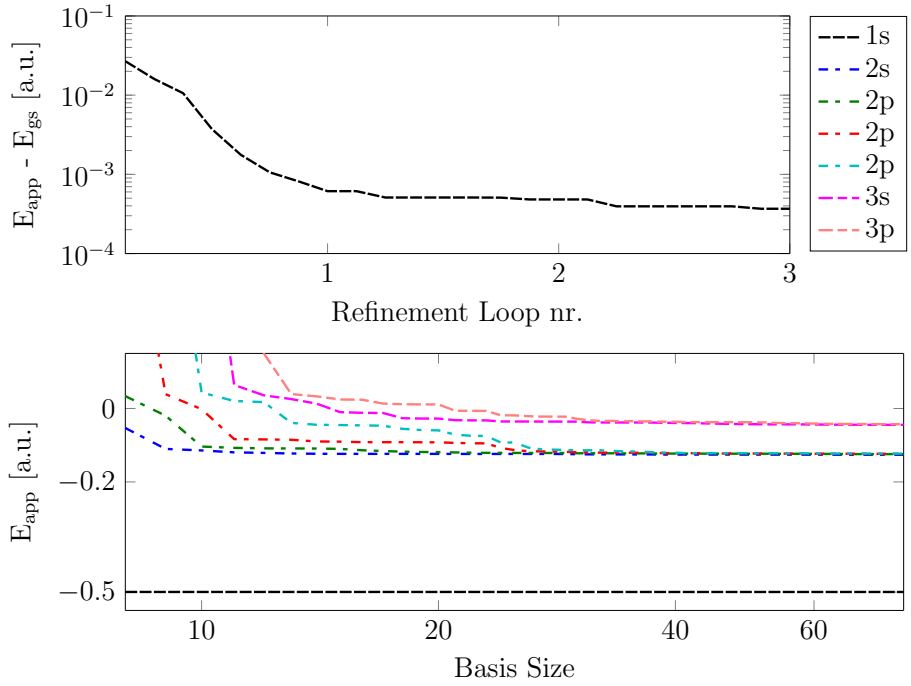

Figure 5.1: *Optimization progress of approximated energy E_{app} for hydrogen. The ground state is improved through refinement loops, while additional basis function are added for improving the exited states.*

functions and trial functions. However, as computations are slow due to the expansion of the Coulomb potential, and the calculations are merely a demonstration of the method, it was not deemed necessary. Lastly, notice how the calculated energy of the 2s state is below the tabulated value. This is theoretically impossible when consulting the *Mini-Max theorem*. However, since the Coulomb potential is an expansion, such small deviations are to be expected.

5.3 Zeeman effect

The degeneration of the exited states can be lifted by applying a magnetic field in one direction, which will select a preferred direction in space of the angular momentum. This is called the *Zeeman effect* and is due to the fields interaction with the magnetic dipole moment of the electron. Pointing the magnetic field in the direction of the

Table 5.1: *Results of first five states from calculations on the hydrogen atom without spin. Tabulated values are calculated from equations in Appendix B.*

State	Quantity	Exp. val. [a.u.]	Result [a.u.]	Rel. deviation
1s	E	-0.5000	-0.4996	$8.00 \cdot 10^{-4}$
	r^2	3	2.992	$2.67 \cdot 10^{-3}$
2s	E	-0.1250	-0.1265	$1.20 \cdot 10^{-2}$
	r^2	42	39.19	$6.69 \cdot 10^{-2}$
2p	E	-0.1250	-0.1246	$3.20 \cdot 10^{-3}$
		-0.1250	-0.1243	$5.60 \cdot 10^{-3}$
		-0.1250	-0.1236	$1.12 \cdot 10^{-2}$
	r^2	30	28.64	$4.53 \cdot 10^{-2}$
		30	28.97	$3.43 \cdot 10^{-2}$
		30	27.36	$8.80 \cdot 10^{-2}$

z-axis of the system will cause the interaction to depend only on the z-component of the angular momentum L_z.

The effect of the magnetic field of strength B can be considered a perturbation to the Hamilton [13]

$$\hat{H}' = \mu_B B \hat{L_z} \ , \tag{5.7}$$

where $\mu_B = \frac{e\hbar}{2m_e}$ is the Bohr magneton. This perturbation can only be regarded as valid for weak magnetic fields, as the dependence on field strength no longer is linear for high magnetic field strength [13]. However, only weak magnetic fields were considered in these calculations.

The calculations were done for a magnetic field of varying strength applied on the same hydrogen model as above. However, only the lowest five states were calculated. Adding the perturbation of the applied magnetic field to the Hamiltonian yields the data displayed in figure 5.2. All the energies are linear in field strength, as described by equation 5.7. Furthermore, the four-fold degeneracy of the first exited state is lifted. As expected no states with zero angular momentum are affected by the magnetic field.
The expectation value of the L_z-operator can be obtained from the

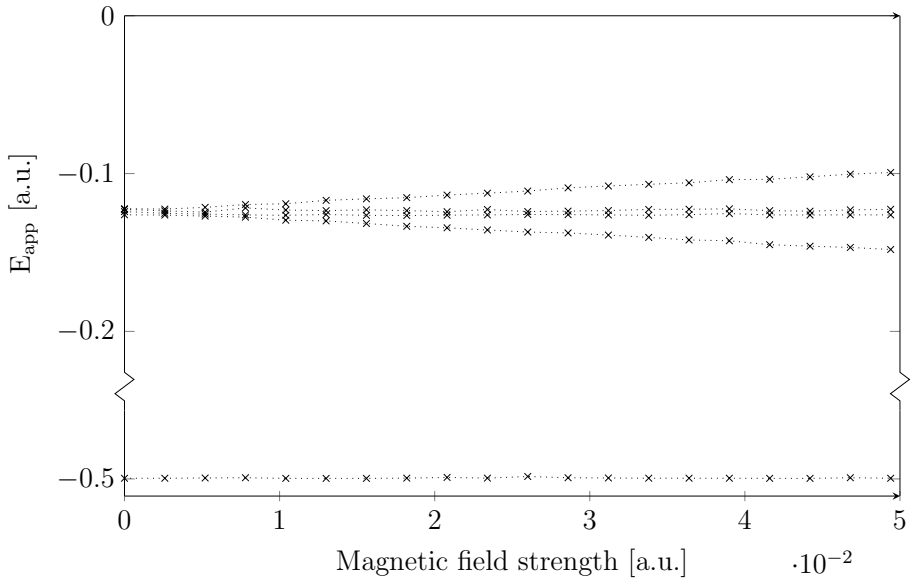

Figure 5.2: *Calculated energies of spinless hydrogen atom affected by magnetic field. The lines are merely for guiding the eye.*

slope $\frac{\Delta E}{\Delta B}$, as the following relation can be deduced from equation 5.7

$$\langle \hat{L_z} \rangle = \frac{\Delta E}{\mu_B \Delta B} \, . \tag{5.8}$$

The estimated values of $\langle \hat{L_z} \rangle$ using equation 5.8 are given in table 5.2 along with the tabulated values.

Table 5.2: *Results from calculations on the hydrogen atom in an external magnetic field.*

State	Quantity	Exp. val. [a.u.]	Result [a.u.]	Rel. deviation
2s	L_z	0	$-8.7 \cdot 10^{-3}$	–
2p	L_z	-1	-0.974	$2.60 \cdot 10^{-2}$
		0	$1.8 \cdot 10^{-2}$	–
		1	0.998	$2.00 \cdot 10^{-3}$

Although the relative deviations of the results from tabulated values are fairly small, a higher precision could be desired. While this

could be achieved by increasing the size of the basis and using more trial functions, it would be extremely time consuming, as both the Coulomb potential and the perturbation has to be calculated for each magnetic field strength. However, as this is merely a demonstration of the method further precision was not deemed necessary.

Chapter 6

Results

All system described in the following chapter consists of bosons, thus their states are not restricted by the Pauli exclusion principle. Furthermore, all particles are of identical mass, m, prompting m as the scale of mass in the calculations. The matrix elements used for the computations are given in Appendix A.

6.1 Squeezing of two-particle systems

As described in section 4.2 only an infinitesimal attraction between the particles should be sufficient to create a bound system in two dimensions. Thus, an interaction potential consisting of a single Gaussian was chosen

$$V_{int,1}(r) = -S_1 \exp\left(-\frac{r^2}{b_{int}^2}\right), \tag{6.1}$$

where r was the distance between the particles, and S_1 is the strength of the potential. b_{int} was defined as the the length scale for the calculations. The strength of the potential was tuned, such that the ground state energy would be zero in three dimension. Thus, as the system transitions into two dimensions, the energy should decrease and the system should become further bound. This was done due to an unfortunate consequence of the Gaussian basis. As the width of the oscillator tends towards larger values, wider Gaussians are needed in order to describe the system. The variational method takes the lowest eigenvalue of the Hamiltonian as the ground state energy, however, the eigenvalue of the widest Gaussian will tend towards zero. This is due to the eigenvalues of the harmonic oscillator having the form $\frac{\hbar^2}{2mb_i^2}$, where b_i is the Gaussian width from equation 3.19. Thus, the approximated energy using Gaussians will not exceed zero when the system is affected by the harmonic oscillator. Tuning the interactive strength led to $S_1 = 2.684$.

In addition to the simple interaction potential described in equation 6.1, another slightly more realistic potential was used

$$V_{int,2}(r) = 2S_2 \exp\left(-\frac{r^2}{(b_{int}/2)^2}\right) - S_2 \exp\left(-\frac{r^2}{b_{int}^2}\right). \tag{6.2}$$

This potential resembles that of atom-atom or nucleon-nucleon interaction, in that it is attractive at short ranges and highly repulsive at very close range. The potential strength S_2 was also tuned for a ground state energy of zero in the limit of three dimensions. This yielded $S_2 = 4.188$.

Lastly the effect of an exponential potential was explored using

$$V_{int,3}(r) = -S_3 \exp\left(-b_{int} r\right), \tag{6.3}$$

where the interactive strength was tuned to $S_3 = 1.4456$.

The results were calculated using an initial basis of 10 Gaussian, which were optimized through three refinement loops with 8000 trial functions for each Gaussian. Thereafter, another six Gaussians were added to the basis, each being selected among 4000 candidates. The calculated binding energies, $\mathrm{E_{app}} - \frac{1}{2}\hbar\omega$, of the two body system for all three interaction potentials can be seen in figure 6.1.

In the three dimensional limit the binding energy asymptotically approaches zero due to the tuning of the strength of the interactive potentials. As the system is squeezed in the z-direction by the harmonic oscillator, the energy drops until the system reaches the two dimensional limit. The energy, which the system reaches upon being squeezed, is dependent on both the tuned strength of the potential and the actual shape of the potential. For instance, the local minimum in the energy for the double Gaussian interaction is due to the shape of the potential. As the particles are squeezed together their expected distance reaches the bottom of the outer Gaussian, while any further squeezing causes less attraction, thus a lesser bound system. Furthermore, the energy during the transition shows high dependence on the reach of the potential. The curves for the three potentials are almost identical for the first part of the transitions, which is due to the potentials appearing identical from large distances. Once the particles are squeezed further together, the difference between the potentials becomes noticeable. For instance, the exponential potential has a longer range than the Gaussian potentials, which causes its

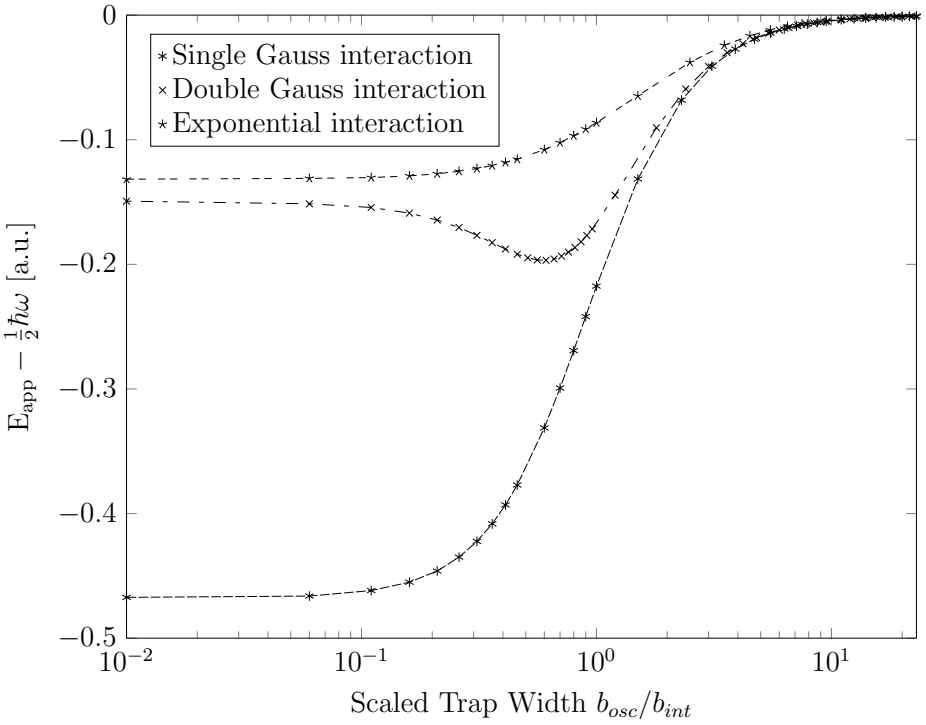

Figure 6.1: *Calculated ground state energy of two particle system for various trap widths. The dashed lines are merely for guiding the eye.*

corresponding curve to break off from the other curves early. From these observations it appears very likely that scaling the potentials according to their effective range might result in a similar, or in best case universal, dimensional crossover.

6.2 Potentials scaled with effective range

In order to compute the effective ranges using equation 4.12 the wave function, u_0, and the free-scattering wave function, $\tilde{u}_0$, had to be found for each potential. The wave function u_0 was found by solving the Schrödinger equation 4.7 for $E = 0$ numerically. The free-scattering wave function was determined as a straight line with the same slope as u_0 for large distances. This was due to $\tilde{u_0}$ being defined

as the function with the same asymptotic behaviour as the wave function. For potentials tuned for zero energy in the three dimensional limit, the asymptotic behaviour of the wave function should be a straight line with zero slope. This is due to the wave functions having the shape $\psi = e^{\sqrt{E_B}rC}$, with E_B being the binding energy, and C being some constant. Thus, a binding energy of zero outside the potential yields a constant wave function. The numerically calculated wave functions can be seen in Appendix C. Inserting the wave functions into equation 4.12 yields the effective ranges displayed in table 6.1 As expected the exponential potential has a much larger effective

Table 6.1: *Calculated effective ranges for interactive potentials.*

Potential	Single Gaussian	Double Gaussian	Exponential
Effective range	1.4394	1.7061	3.5483

range than the Gaussian potentials. Likewise, the two Gaussian potentials have very similar effective ranges with the double Gaussian having the largest, which is probably due to the tuned strength of this potential having the highest value.

For scaling the calculated result in figure 6.1 the length scale of individual curves was chosen as the corresponding effective range. Thus, the curves are plotted as a function of the harmonic oscillator width in units of the respective effective ranges. Furthermore, the energy is scaled according to the natural unit of energy with the chosen scales of length and mass. Hence, the energy is given in units of $\frac{\hbar^2}{2\mu R^2}$, where R corresponds to the effective effective range of the individual curves. The result of the scaling can be seen in figure 6.2. As a result of the scaling the curves seem to follow a universal curve during the weak-binding part of the dimensional crossover. Whereas the curve of the exponential interaction broke off from the other curves very early in figure 6.1, it now follows the same path as the Gaussian potentials, even though the shape of the potentials is different. In the two dimensional limit the curves are obviously very different, as the values, which the curves converge towards, are highly dependent on the tuning of the potentials as well as their shape. Scaling the curves has resulted in a different ordering of which potential yields the tightest bound system. However, no useful information has come of this, as the actual crossover rather than the two dimensional limit

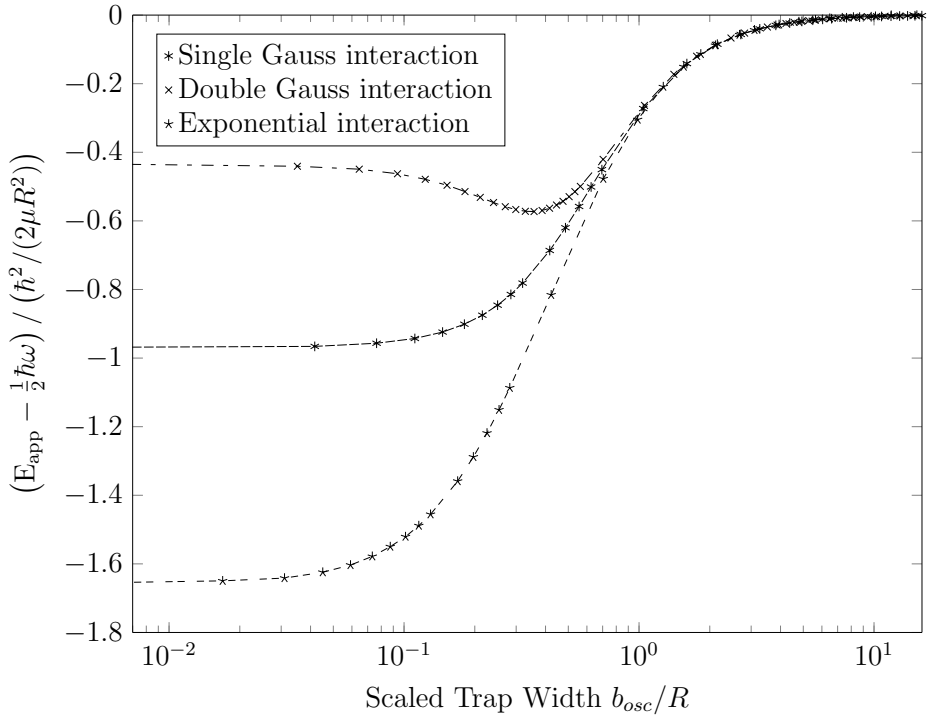

Figure 6.2: *Results from figure 6.1 scaled according to the effective ranges, R, of the interactive potentials.*

is of interest. Figure 6.3 shows a comparison of figure 6.1 and figure 6.2 in the area of interest, which is during the dimensional crossover. The curves all tend asymptotically towards zero due to the tuning of the potentials, whereby the universality of the curves in both the scaled and the non-scaled case should come as no surprise. However, as figure 6.3 clearly shows, the non-scaled curves starts diverging from each other as soon as the oscillator width becomes comparable with the length scale. However, this is not the case of the scaled curves, which diverge by only a tiny fraction once the oscillator width becomes equal to the length scale. Although this example is not proof of a universal behaviour during the dimensional crossover, the results highlighted in figure 6.3 clearly suggest a universal behaviour.

This illustrates the possibility of a universality of the dimensional crossover for two-particle bosonic systems. Whether this universality applies to systems of any number of particles is left to explore. Although the fully correlated Gaussian method was excellent for ap-

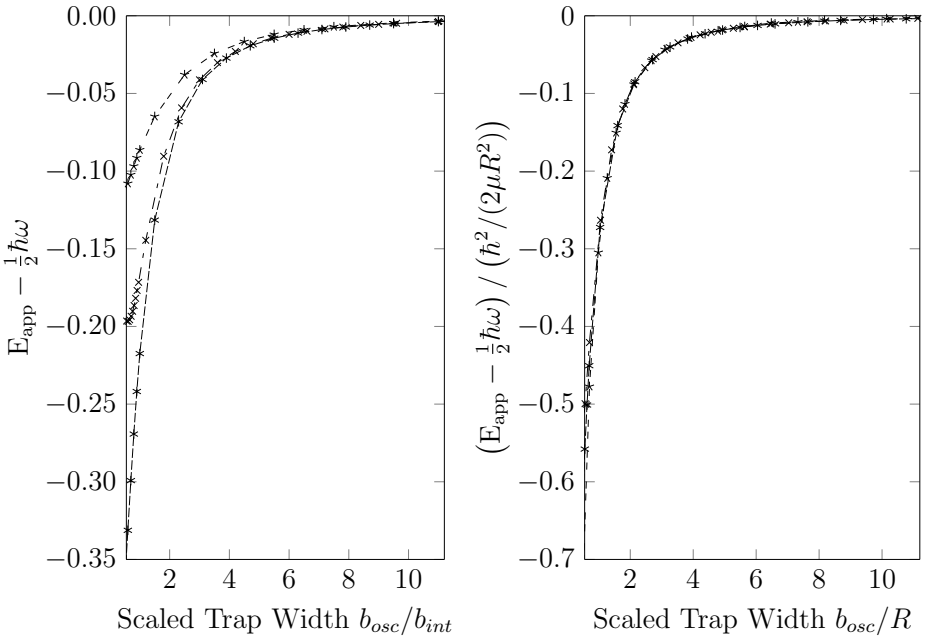

Figure 6.3: *Comparison of dimensional crossover displayed in figure 6.1 and figure 6.2.*

proximating energies for two particles, it struggled at three particles, due to the large increase in parameters when considering all three spacial dimensions. Thus, a more refined algorithm than simply choosing random trial functions is required for describing more particles. Furthermore, an uneven distribution of mass may also affect the crossover, all of which could be explored in further studies.

Chapter 7

Conclusion

The objective of this thesis was to explore the dimensional crossover from three to two dimensions. In order to achieve this, stochastic variational method was used with a basis of fully correlated Gaussians. The consequences of using fully correlated Gaussians were discussed, and their ability to describe non-spherical symmetric systems was tested by calculating the spectrum of hydrogen and the splitting of energies when applying a magnetic field to the spinless hydrogen atom. The results confirmed the ability of the basis to describe non-spherical symmetric systems.

For realising the transition of dimensionality, a two boson system was put in a one dimensional harmonic oscillator trap. By squeezing the oscillator, the movement of the particles became confined in one dimension, thus effectively restricting the particles to two dimensional space. In two dimensions the centrifugal barrier operator has negative eigenvalue, causing an infinitesimal attraction between the particles to create a bound system. Using the fully correlated Gaussian method, the ground state energy was calculated for various widths of the trap. This was done for three different kinds of interactive potentials between the particles in order to illustrate their effect on the dimensional crossover. As expected the energy of the system decreased when being squeezed. However, the energy curves were very dependent on the shape and strength of the interactive potential. Nevertheless, the initial part of the transition was identical for all potentials, which prompted an investigation of whether scaling the curves according to some physical parameter would result in a universal curve. Thus, the effective ranges of the potentials were calculated numerically and used as the length scale of the calculations. The result revealed that the weak-binding part of the transition was universal for all three interactive potentials.

Further studies could explore the effect of adding more particles to the system as well as using particles, which are not identical.

Bibliography

[1] Bellotti, F. F.: *Two- and Three-Dimensional Few-Body Systems in the Universal Regime*, PhD thesis, IFA, Aarhus University, 2014, arXiv:1411.2937

[2] Suzuki, Y., Varga, K.: *Stochastic Variational Approach to Quantum-Mechanical Few-Body Problems*, Springer, Inc., 1998

[3] University of California, Berkeley: *Gram matrix* `https://inst.eecs.berkeley.edu/ ee127a/book/login/def_Gram_matrix.html`

[4] Wikibooks: *Correlated Gaussian method in Quantum Mechanics* `http://en.wikibooks.org/wiki/Correlated_Gaussian_method_in_Quantum_Mechanics`

[5] Sørensen, H. H.: *Correlations in many-body systems with the Stochastic Variational Method*, Master's thesis, IFA, Aarhus University, 2005 `http://arxiv.org/pdf/cond-mat/0502126.pdf`

[6] Fedorov, D. V.: *Yet Another Introduction to Numerical Methods* `http://owww.phys.au.dk/ fedorov/Numeric/now/Book/main.pdf`

[7] Martin, B. R.: *Nuclear and Particle Physics*, 2nd Ed., John Wiley & Sons Ltd, 2009

[8] Milonni, P. W., Eberly, J. H.: *Laser Physics*, John Wiley & Sons Ltd, 2010

[9] Fedorov, D. V.: Personal communication, May 6, 2016

[10] Siemens, P. J., Jensen, A. S.: *Elements of Nuclei: Many-body Physics With The Strong Interaction*, Addison-Wesley Publishing Company, Inc., 1987

[11] Griffiths, D. J.: *Introduction to Quantum Mechanics*, 2nd Ed., Pearson, 2005

[12] Taasti, V. T.: *Quantums States with High Angular Momentum in Correlated Gaussian Basis*, Bachelor's thesis, IFA, Aarhus University, 2012
`http://users-phys.au.dk/fedorov/bachelor/vicki-taasti-high-momentum.pdf`

[13] Demtröder, W.: *Atoms, Molecules and Photons*, 2nd Ed., Springer, Inc., 2010

Appendix A

Full correlation matrix elements

This appendix will list the matrix elements used in the numerical computation. For this some notation has to be introduced. A basis function will be denoted

$$|A, s; x\rangle \equiv \exp\left(-\sum_{i,j=1}^{D\cdot n} A_{ij}(\tilde{\boldsymbol{x}}_i - \tilde{\boldsymbol{s}}_i)(\tilde{\boldsymbol{x}}_j - \tilde{\boldsymbol{s}}_j)\right) = e^{-(\tilde{\boldsymbol{x}}-\tilde{\boldsymbol{s}})^T A(\tilde{\boldsymbol{x}}-\tilde{\boldsymbol{s}})}\,, \tag{A.1}$$

where the tilde denotes super vectors. For more simplistic expressions for integrals the following notation is used

$$\mathrm{d}\tilde{\boldsymbol{x}} \equiv \mathrm{d}^D\boldsymbol{x}_1 \ldots \mathrm{d}^D\boldsymbol{x}_n\,, \tag{A.2}$$

where D is the amount of spatial dimensions. For this entire thesis $D = 3$ was used.
Formulae used to calculate matrix elements were found in [4], however, all elements are analytical and can be calculated using the described integrals.

A.1 Overlap and kinetic energy

The overlap of correlated Gaussian functions is given as

$$\begin{aligned} N &\equiv \langle A', s'; x'|A, s; x\rangle \\ &= \int_{-\infty}^{\infty} \mathrm{d}\tilde{\boldsymbol{x}}\; e^{-(\tilde{\boldsymbol{x}}-\tilde{\boldsymbol{s}}')^T A'(\tilde{\boldsymbol{x}}-\tilde{\boldsymbol{s}}')-(\tilde{\boldsymbol{x}}-\tilde{\boldsymbol{s}})^T A(\tilde{\boldsymbol{x}}-\tilde{\boldsymbol{s}})} \\ &= \frac{\pi^{\frac{D\cdot n}{2}}}{\sqrt{\det B}}\; e^{-\tilde{\boldsymbol{s}}'^T A'\tilde{\boldsymbol{s}}'-\tilde{\boldsymbol{s}}^T A\tilde{\boldsymbol{s}}+\frac{1}{4}\tilde{\boldsymbol{v}}^T B^{-1}\tilde{\boldsymbol{v}}}\,, \end{aligned} \tag{A.3}$$

where

$$B \equiv A + A' \tag{A.4}$$

$$\tilde{\boldsymbol{v}} \equiv 2A\tilde{\boldsymbol{s}} + 2A'\tilde{\boldsymbol{s}}'\,. \tag{A.5}$$

Following this the expectation value of the kinetic energy is given as

$$\begin{aligned} T \equiv & \langle A', s'; x' | \frac{\partial^T}{\partial \tilde{\boldsymbol{x}}} \Lambda \frac{\partial}{\partial \tilde{\boldsymbol{x}}} | A, s; x \rangle \\ = & N \cdot \left(2\mathrm{tr}\left(A' \Lambda A B^{-1} \right) + 4 \tilde{\boldsymbol{u}}^T A' \Lambda A \tilde{\boldsymbol{u}} \right. \\ & \left. - 4 \tilde{\boldsymbol{u}}^T \left(A' \Lambda A \tilde{\boldsymbol{s}} + A \Lambda A' \tilde{\boldsymbol{s}'} \right) + 4 \tilde{\boldsymbol{s}'}^T A' \Lambda A \tilde{\boldsymbol{s}} \right) , \end{aligned} \tag{A.6}$$

where Λ is the reduced mass matrix described in equation 3.16 and

$$\tilde{\boldsymbol{u}} = \frac{1}{2} B^{-1} \tilde{\boldsymbol{v}} \, . \tag{A.7}$$

A.2 Coulomb potential

As stated previously the coulomb interaction can be described through an expansion of Gauss functions. Thus, the Coulomb interaction between particle i and j is given as

$$\hat{V}_{coul,ij} \; = \; q_i q_j \sum_{k=1}^{G} \beta_k \cdot \exp\left(\frac{(\boldsymbol{r}_i - \boldsymbol{r}_j)^2}{\alpha_k^2} \right) \tag{A.8}$$

Using the inverse of the coordinate transformation matrix $\mathcal{U}^{-1}$ allows a description of the potential energy operator using Jacobi coordinates.

$$\begin{aligned} \hat{V}_{coul,ij} \; & = q_i q_j \sum_{k=1}^{G} \beta_k \cdot \exp\left(\frac{\boldsymbol{r}_i^2 + \boldsymbol{r}_j^2 - 2\boldsymbol{r}_i \cdot \boldsymbol{r}_j}{\alpha_k^2} \right) \\ & = q_i q_j \sum_{k=1}^{G} \beta_k \cdot \exp\left(\frac{\tilde{\boldsymbol{r}}^T R_{ij} \tilde{\boldsymbol{r}}}{\alpha_k^2} \right) \\ & = q_i q_j \sum_{k=1}^{G} \beta_k \cdot \exp\left(\tilde{\boldsymbol{x}}^T \kappa_{ijk} \tilde{\boldsymbol{x}} \right) , \end{aligned} \tag{A.9}$$

where q_i is the charge of the i'th particle. R_{ij} denotes the interaction

matrix between particle i and j, which takes the form

$$R_{ij} = \begin{array}{c} \\ 1 \\ i \\ j \\ \vdots \\ n \end{array} \begin{array}{c} \begin{array}{ccccc} 1 & i & j & \dots & n \end{array} \\ \begin{pmatrix} 0_D & 0_D & 0_D & \dots & 0_D \\ 0_D & I_D & -I_D & \dots & 0_D \\ 0_D & -I_D & I_D & \dots & 0_D \\ \vdots & \vdots & \vdots & \ddots & \vdots \\ 0_D & 0_D & 0_D & \dots & 0_D \end{pmatrix} \end{array}, \tag{A.10}$$

where 0_D is the zero matrix and I_D is the identity matrix both of side length D. Following this κ_{ijk} is defined as

$$\kappa_{ijk} \equiv \mathcal{U}^{-1^T} \frac{R_{ij}}{\alpha_k^2} \mathcal{U}^{-1} . \tag{A.11}$$

Using this definition the potential energy matrix element can be computed in the same manner as the overlap:

$$\begin{aligned} V_{coul,ij} &\equiv \langle A', s'; x' | \hat{V}_{coul,ij} | A, s; x \rangle \\ &= q_i q_j \sum_{k=1}^{G} \beta_k \frac{\pi^{\frac{D \cdot n}{2}}}{\sqrt{\det \kappa_{ijk}}} e^{-\tilde{\boldsymbol{s}}'^T A' \tilde{\boldsymbol{s}}' - \tilde{\boldsymbol{s}}^T A \tilde{\boldsymbol{s}} + \frac{1}{4} \tilde{\boldsymbol{v}}^T \kappa_{ijk}^{-1} \tilde{\boldsymbol{v}}} \end{aligned} \tag{A.12}$$

A.3 Angular momentum

For this matrix element only the two particle case is considered. Thus, the matrices A will be of dimensions 3×3 and the Jacobi coordinates read

$$\tilde{\boldsymbol{x}} = \boldsymbol{x} = \begin{pmatrix} x_x \\ x_y \\ x_z \end{pmatrix} . \tag{A.13}$$

Applying the z-component of the angular momentum operator on a Gaussian function yields

$$\begin{aligned} \hat{L_z} | A, s; x \rangle = \big(& x_y (2A_{11} x_x - 2u_x + A_{12} x_y + A_{21} x_y + A_{13} x_z + A_{31} x_z) \\ & - x_x (A_{12} x_x - 2u_y + A_{21} x_x + 2A_{22} x_y + A_{23} x_z + A_{32} x_z) \big) \\ & \cdot | A, s; x \rangle , \end{aligned} \tag{A.14}$$

where $\boldsymbol{u} = 2\boldsymbol{s}^T A$ is three dimensional such as A.13. The above expression can be reduced since A is symmetric. In matrix form equation A.14 reads

$$\hat{L_z}|A, s; x\rangle \;=\; \left(\boldsymbol{x}^T F \boldsymbol{x} + \boldsymbol{a}^T \cdot \boldsymbol{x}\right)|A, s; x\rangle \;, \tag{A.15}$$

where

$$F \;=\; \begin{pmatrix} -2A_{12} & A_{11} - A_{22} & -A_{23} \\ A_{11} - A_{22} & 2A_{12} & A_{13} \\ -A_{23} & A_{13} & 0 \end{pmatrix} \text{ and } \boldsymbol{a} \;=\; \begin{pmatrix} 2u_y \\ -2u_x \\ 0 \end{pmatrix} . \tag{A.16}$$

Thus, the expectation value of the operator in matrix form is given as

$$\langle A', s'; x|\hat{L_z}|A, s; x\rangle \;=\; N\left(\boldsymbol{u}^T F \boldsymbol{u} + \frac{1}{2}\mathrm{tr}(FB^{-1}) + \boldsymbol{a}^T \boldsymbol{u}\right) \tag{A.17}$$

A.4 Harmonic oscillator

For a system consisting of two identical particles of mass m the potential energy operator of a harmonic oscillator can be written as

$$\begin{aligned} V_{osc} =& \frac{1}{2}\frac{\hbar^2}{m b_{osc}^4} z_1^2 + \frac{1}{2}\frac{\hbar^2}{m b_{osc}^4} z_2^2 \\ =& \frac{1}{2}\frac{\hbar^2}{m b_{osc}^4}\left(\frac{(z_1 - z_2)^2}{2} + \frac{(z_1 + z_2)^2}{2}\right) \\ =& \frac{1}{2}\frac{\hbar^2}{\frac{1}{2} m b_{osc}^4} x_z^2 + \frac{1}{2}\frac{\hbar^2}{2 m b_{osc}^4} R_z^2 \\ =& \frac{1}{2}\mu\omega_\mu^2 x_z^2 + \frac{1}{2} M \omega_M^2 R_z^2 \,, \end{aligned} \tag{A.18}$$

where μ and ω_μ are the reduced mass and its corresponding oscillation frequency, while M and ω_M are the total mass and its corresponding oscillation frequency. Lastly x_z is the z-component of the relative coordinate, while R_z is the z-component of the center of mass coordinate. Thus, the potential energy operator can be split into a relative part and a center of mass part.
The expectation value is calculated as

$$\langle A', s'; x|\hat{V_{osc}}|A, s; x\rangle \;=\; N\left(\boldsymbol{u}^T Q \boldsymbol{u} + \frac{1}{2}\mathrm{tr}(QB^{-1})\right) \;, \tag{A.19}$$

where Q is the matrix

$$Q = \begin{pmatrix} 0 & 0 & 0 \\ 0 & 0 & 0 \\ 0 & 0 & 1 \end{pmatrix} , \tag{A.20}$$

which selects the z-component of the two particle jacobi coordinate.

Appendix B

Expectation values of hydrogen

The following equations were used for calculating the tabulated expectation values for the hydrogen atom:

$$E_n = -\frac{m_e e^4}{2(4\pi\epsilon_0)^2\hbar^2 n^2} \tag{B.1}$$

$$\langle\hat{r}^2\rangle = a_0^2 n^4 \left(1 + \frac{3}{2}\left(1 - \frac{l(l+1) - \frac{1}{3}}{n^2}\right)\right) \tag{B.2}$$

$$\langle\hat{L_z}\rangle = m\hbar \ , \tag{B.3}$$

where n is the principal quantum number, m_e is the mass of the electron, l is the angular quantum number, and m is the magnetic quantum number.

Appendix C

Zero energy scattering wave functions

The following figures show the results from solving equation 4.7 numerically for $E = 0$. The free-scattering wave function $\tilde{u}_0(r)$ is equal to the asymptotic behaviour of the wave function $u_0(r)$. Due to the binding energy being zero outside the potential, the resulting free-scattering wave function is a straight line with zero slope. Using these wave functions the effective ranges were calculated.

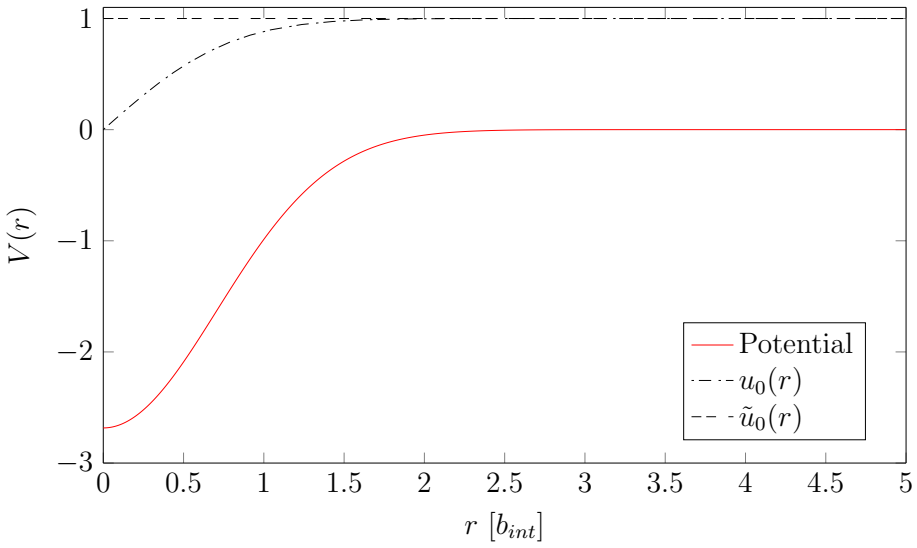

Figure C.1: *Numerically calculated wave functions for the single Gaussian potential described in equation 6.1. The normalized wave function, u_0, and free-scattering wave function, $\tilde{u}_0$, are plotted alongside the corresponding potential.*

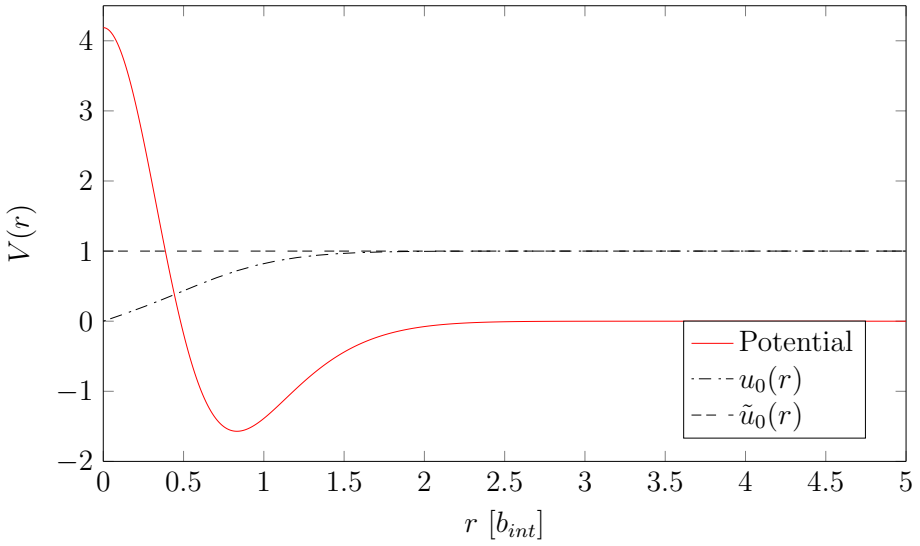

Figure C.2: *Numerically calculated wave functions for the double Gaussian potential described in equation 6.2. The normalized wave function, u_0, and free-scattering wave function, $\tilde{u}_0$, are plotted alongside the corresponding potential.*

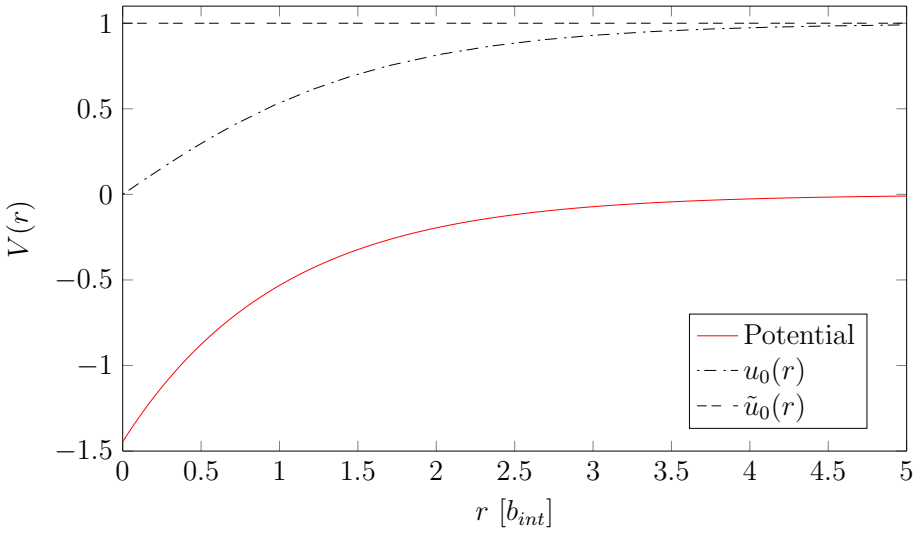

Figure C.3: *Numerically calculated wave functions for the exponential potential described in equation 6.3. The normalized wave function, u_0, and free-scattering wave function, $\tilde{u}_0$, are plotted alongside the corresponding potential.*